BRITISH JOURNAL OF HOSPITAL MEDICINE

ARTICLE

Early Prediction of Death Risk in Progressive Nasopharyngeal Carcinoma Using Radiomics Nomogram Based on Clinical Semantic Multi-Parameter Magnetic Resonance Imaging

Yuzhen Xi[1], Yuanhui Ding[2], Yingjiao Zhang[3], Mengze Wang[4], Chunying Wu[5], Xuan Chen[1], Lei Ruan[4], Zhongxiang Ding[5], Feng Jiang[6,*], Miao Liu[1,*]

[1]Department of Radiology, 903th RD Hospital of PLA, Hangzhou, Zhejiang, China
[2]Department of Radiology, People's Hospital of Wuxing District, Maternal and Child Health Hospital of Wuxing District, Huzhou, Zhejiang, China
[3]Department of Gastroenterology, 903th RD Hospital of PLA, Hangzhou, Zhejiang, China
[4]Department of Radiology, Zhejiang Cancer Hospital, Hangzhou, Zhejiang, China
[5]Department of Radiology, Affiliated Hangzhou First People's Hospital, Westlake University School of Medicine, Hangzhou, Zhejiang, China
[6]Department of Head and Neck Radiotherapy, Zhejiang Cancer Hospital, Hangzhou, Zhejiang, China
*Correspondence: jiangfeng@zjcc.org.cn (Feng Jiang); xhqqbliumiao@163.com (Miao Liu)

Abstract

Aims/Background Patients with recurrent or/and metastatic nasopharyngeal carcinoma (NPC) have a notably low survival rate. Our primary objective in this study is to establish a comprehensive nomogram model based on clinical factors, semantic features, and multi-parameter magnetic resonance imaging (MRI) radiomic features, and to predict the risk of mortality in patients with progressive NPC following intensity-modulated radiation therapy.

Methods A retrospective study, including 110 patients with recurrent or/and metastatic NPC who underwent treatment at the Zhejiang Cancer Hospital between June 2012 and December 2016, was conducted. Comprehensive reviews of clinical and pre-treatment MRI data were undertaken. Patients were categorized into two groups based on their mortality status within a 5 year-frame: the non-death group (54 cases) and the death group (56 cases). Radiomic features were extracted from patients' MRIs and the best feature set was selected. Each patient was assigned a radiomic score (Rad-Score). A combined model was constructed using multivariate binary logistic regression, incorporating Rad-Score, semantic features, and clinical data. Receiver operating characteristic (ROC) curves and calibration plots were generated to evaluate the predictive performance of the radiomic feature model, the clinical-semantic feature model, and the combined model for predicting death risk in patients with progressive NPC. A nomogram based on the combined model was constructed.

Results Gender, invasion of the carotid sheath by the primary tumour, tumour volume, and progression time showed statistically significant differences between the two groups ($p < 0.05$). There were statistically significant differences between the three models in the death and non-death groups ($p < 0.001$). The area under the curve (AUC) value for the radiomic feature model was 0.861 (95% confidence interval [CI]: 0.783–0.920), while the AUC value for the clinical-semantic feature model was 0.797 (95% CI: 0.709–0.868). The combined model demonstrated the highest efficacy for predicting death risk in NPC patients, with an AUC value of 0.904 (95% CI: 0.832–0.952), accuracy of 0.818, sensitivity of 0.857, specificity of 0.870, negative predictive value of 0.778, and positive predictive value of 0.857.

Conclusion The combined model incorporating clinical features, semantic features and multi-parameter MRI radiomic features is a highly valuable tool for predicting death risk in patients with progressive NPC, providing a quantitative approach to aiding in early clinical intervention and treatment.

Key words: nasopharyngeal carcinoma; machine learning; nomogram; mortality

Submitted: 17 September 2024 Revised: 29 November 2024 Accepted: 12 December 2024

How to cite this article:
Xi Y, Ding Y, Zhang Y, Wang M, Wu C, Chen X, Ruan L, Ding Z, Jiang F, Liu M. Early Prediction of Death Risk in Progressive Nasopharyngeal Carcinoma Using Radiomics Nomogram Based on Clinical Semantic Multi-Parameter Magnetic Resonance Imaging. Br J Hosp Med. 2025. https://doi.org/10.12968/hmed.2024.0658

Introduction

Nasopharyngeal carcinoma (NPC) is an etiologically heterogeneous malignancy originating from the epithelium of the nasopharyngeal mucosa, exhibiting heightened sensitivity to radiation therapy (de Martel et al, 2020). Given the higher susceptibility to tumourigenesis and the restricted access of nasopharynx to surgical treatment due to its anatomical location, radiation therapy stands as the primary treatment modality for non-metastatic NPC patients (Sung et al, 2021). Progressive advancements in medical equipment and the development of radiotherapy technology have refined intensity-modulated radiation therapy (IMRT) into a comprehensive treatment, which currently is the primary treatment method, with a favourable prognostic outcome in NPC patients and an ability to elevate overall survival (OS) rate to over 80% (Chen et al, 2022). During recurrence or distant metastasis, however, the use of first-line medication does not seem to provide much protection, given the outcome statistics obtained from a previous report: a median post-treatment progression-free survival duration of only ~7 months, a 5-year OS rate of <20%, and a mortality rate as high as 91% in patients with NPC metastasis (Siak et al, 2021). Hence, there exists a need to unravel the survival among patients experiencing NPC relapse and metastasis.

Recent studies have shown that the anatomical-based tumour node metastasis (TNM) staging system lacks precision in guiding clinical practice (Zhuo et al, 2019; Ren et al, 2017; Wu et al, 2021; Zhang et al, 2019). Nonetheless, accurate staging remains crucial for achieving a lower mortality rate in NPC patients (Miao et al, 2022). Patients at risk of death may face a poor prognosis due to delayed intensified treatment, while others may encounter suboptimal outcomes from initial radiotherapy and chemotherapy, resulting in poor compliance and tolerance with subsequent treatment, culminating in death. Although early recurrent patients may benefit from the removal of radiation-resistant tumours, the majority of recurrent cases are diagnosed at an advanced stage (Deng et al, 2023; Tian et al, 2022). Thus, early accurate stratification and intervention emerge as crucial strategies for extending the lifespan of NPC patients, playing a core role in their clinical management. Toumi et al (2021) found that early recurrence of NPC (<2 years) significantly alters survival rates, suggesting a more aggressive nature in tumours that recur sooner. The involvement of the carotid sheath in primary tumour extension or metastatic lymph node invasion has been consistently identified as a significant prognostic factor in NPC (Chan et al, 2018; Qiu et al, 2023). In recent years, radiomics as a popular method for studying tumour heterogeneity, has shown higher value than TNM staging in various studies related to risk stratification, recurrence and distant metastasis prediction, and survival application in NPC (Yang et al, 2019; Xi et al, 2022). Previous studies have focused on recurrent or metastatic NPC, with long-term survival of more than 50% in some cases of NPC progression. In recent years, nomograms have been used to construct prediction models as prognostic assessment tools for tumours in various studies. Conceptually, nomograms integrate multiple prognostic and determinant variables, allowing personalized identification and stratification of risk factors (Liu et al, 2023; Xiang et al, 2024).

Magnetic resonance imaging (MRI), as the most essential imaging tool for NPC TNM staging, also serves as a critical non-structured data source for NPC (Qiang et al, 2021). This study aims to integrate clinical and MRI semantic features of progressive NPC with multi-parameter MRI radiomics features to construct a model combining both clinical-semantic and radiomic features. This model predicts the 5-year mortality rate, providing a more accurate patients stratification and a quantitative basis for formulating of treatment plans in clinical practice.

Methods

Clinical Cases

Patient data were derived from 517 cases of pathologically confirmed NPC stage I–IVa treated at the Zhejiang Cancer Hospital from June 2012 to December 2016. The inclusion criteria are as follows: (1) patients with biopsy-proven NPC; (2) individuals diagnosed with stage I–IVa according to the 8th edition of the 2017 American Joint Committee on Cancer (AJCC) staging system, with recurrence and/or distant metastasis within 5 years (Huang and O'Sullivan, 2017); (3) patients aged 18 years or older and receiving complete IMRT treatment; and (4) patients with tumour-type NPC showing no significant artifacts from pre-treatment MRI scans including T1 weighted imaging (T1WI), fat suppressed T2 weighted imaging (FS T2WI) and fat suppressed contrast enhanced-T1 weighted imaging (FS CE-T1WI). Individuals with the following criteria were excluded from the study: (1) comorbidity with other tumours; (2) incomplete treatment; (3) lost to follow-up for 60 months; (4) unqualified magnetic resonance (MR) images; (5) non-mass type NPC; (6) non-progressors; (7) death not caused by progression. Patients with ongoing progression after treatment were not included in our study. Finally, 110 patients with locally advanced NPC were selected. The workflow depicting the patient selection and grouping process is shown in Fig. 1.

The data collected from patients with NPC include gender, age, histopathological type, T stage, N stage, induction chemotherapy regimen and duration, concurrent chemotherapy duration, tumour volume, and time of first detection of recurrence and/or distant metastasis.

Treatment and Follow-Up

Following the completion of IMRT, patients underwent regular follow-ups, with intervals of every 3 months for the first years, followed by semi-annual checks during the second year and annual visits in the subsequent years. The endpoint was the 5-year mortality rate for all patients experiencing recurrence and/or metastasis. The calculation of the endpoint commenced from the day of the initial treatment, considering the first defined event or the last follow-up visit. The last follow-up date for this study was 23 February 2023 (Xi et al, 2024).

MRI Examination Methods

MR scanners Siemens Magnetom Symphony 1.5T (23709, Siemens Medical Solutions, St. Paul, MN, USA) and Siemens Verio 3.0T (40689, Siemens Medical Solutions, Erlangen, Bavaria, Germany) were used for acquiring MR images.

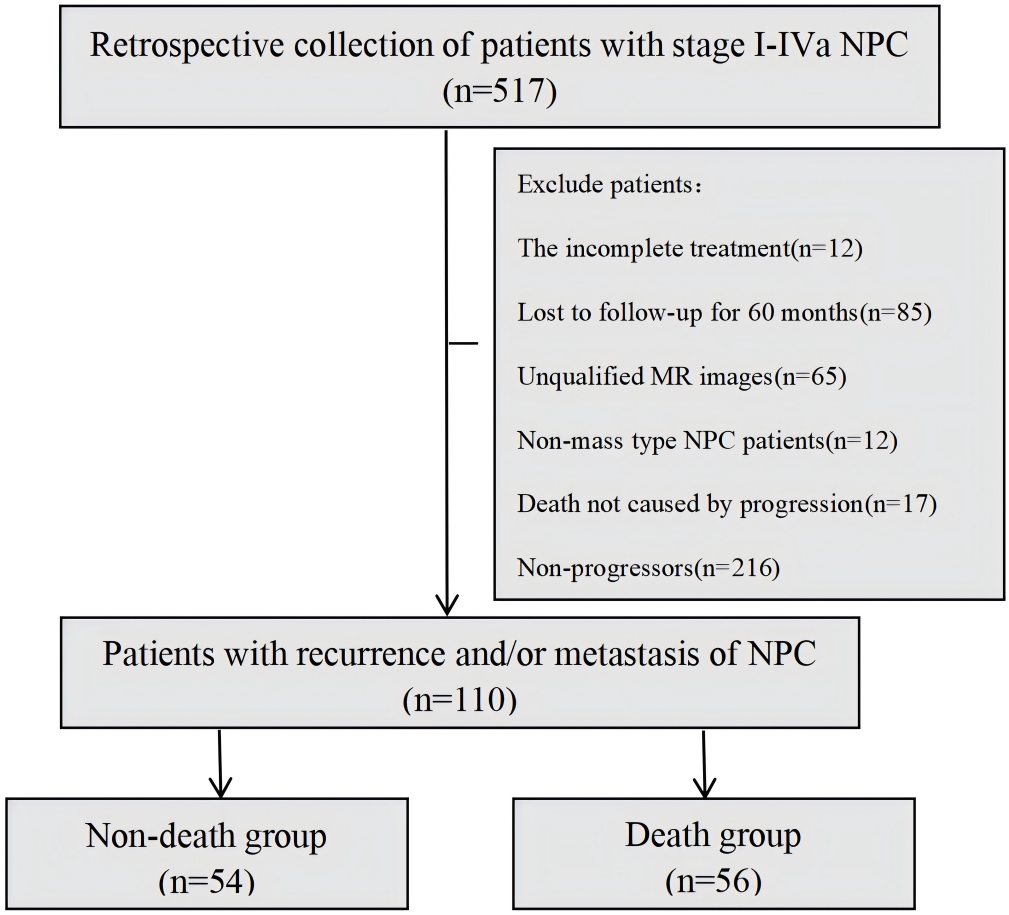

Fig. 1. Flowchart depicting processes of patient selection and categorization into death and non-death groups. From the final selection of 110 eligible cases, 54 cases were categorized into the non-death group and 56 cases in the death group. NPC, nasopharyngeal carcinoma.

Cross-sectional T1WI and FS T2WI were initially acquired. Subsequently, axial FS CE-T1WI images were taken after receiving a dosage of 0.01 mmol/kg gadolinium-based contrast agent. The main components in the scan images are as follows: Axial T1WI: repetition time/echo time (TR/TE) 1700–1800 ms/910 ms, 90° flip angle, 256 × 168 matrix, 5.00 mm slice thickness, and 1.00 mm slice spacing; Axial fs T2WI: TR/TE 5700–6360 ms/4990 ms, with flip angle, matrix, slice thickness, and spacing similar to those of axial T1WI; Axial fs CE-T1WI: TR/TE 450–600 ms/8.89 ms, with flip angle, matrix, slice thickness, and slice spacing similar to those of axial T1WI (Xi et al, 2024).

MR Image Semantic Features

All MR images were obtained before treatment and independently reviewed by two radiologists specialized in head and neck radiology, who had 9 and 16 years of experience, respectively. We took into account patient data such as such as the research criteria for carotid sheath involvement (Qiu et al, 2023; Quan et al, 2022). Nasopharyngeal carcinoma invasion to carotid sheath and neck lymph nodes were studied. A Kappa test was conducted to assess the inter-rater agreement and calculate the kappa coefficient.

NPC Tumour Segmentation, Radiomic Feature Extraction and Selection

The MRI preprocessing and image segmentation protocols encompass the following: (1) Pre-treatment nasopharyngeal MR scans for each case were exported in digital imaging and communications in medicine (DICOM) format. (2) The DICOM-format images were imported into ITK-SNAP software. ITK-SNAP is a free, open-source, multi-platform software application used to segment structures in 3D and 4D biomedical images (http://www.itksnap.org, version 3.8.0). It was originally developed at the University of North Carolina by student teams led by Guido Gerig (NYU Tanden School of Engineering). Two attending radiologists with vast experience in head and neck radiology manually segmented the primary NPC tumour on T1WI, FS T2WI, and FS T1WI+C sequences slice by slice. The segmented tumour was then saved as a region of interest (ROI), and the tumour volume, within-group and between-group correlation coefficients (ICC) were recorded to evaluate inter-observer and intra-observer consistency.

In the image preprocessing, radiomic feature extraction, and selection, the original and outline ROIs were entered into the uAI Research portal (version 3.7.3, United Imaging Intelligence, Shanghai, China). Normalization was first done on them, and then radiomic features were extracted, including First Order, Shape, Gray Level Run Length Matrix (GLRLM), Gray Level Dependence Matrix (GLDM), Gray Level Co-occurrence Matrix (GLCM), Neighborhood Gray Tone Difference Matrix (NGTDM), and Gray Level Size Zone Matrix (GLSZM). Filters, such as original, wavelet, and Laplacian of Gaussian (LoG), were used to obtain 2286 features from sequences (Xi et al, 2024). To maintain image quality across various gadgets, MaxAbsScaler was utilized to preprocess dataset prior to selecting relevant attributes and preserving that above threshold (0.75). Maximum relevance minimum redundancy (mRMR) was used to select 20 features most relevant to the labels and have minimal redundancy. Subsequently, least absolute shrinkage and selection operator (LASSO) regression was applied for dimension reduction, obtaining radiomics signature parameters termed Rad-Score. The predictive model was trained and validated using five-fold cross-validation. Finally, the area under the receiver operating characteristic (ROC) area under curve (AUC) of the radiomic feature model was determined.

Model Estimation, Validation, and Statistical Analysis

The statistical analyses were performed with MedCalc statistical software (version 19.1, MedCalc Software Ltd., Ostend, Belgium) and R software (version 4.2.1, R Core Team, https://cran.r-project.org/src/base/R-4). MedCalc is a statistical software designed specifically for biomedical applications. First, the data were tested for normality. Owing to a dataset of 110 subjects filled with continuous, categorical and rank variables, we used the Kolmogorov-Smirnov test for normality testing. Student's *t*-test was used for normally distributed data, whereas the Mann-Whitney U test was used for non-normally distributed continuous data. The chi-square test was used for qualitative variables and rank variables to analyze whether there were statistically significant differences. If the number of cases with a theoretical frequency $T < 1$ or $1 \leq T \leq 5T$ exceeds one-fifth of the total, Fisher's exact test

was used instead. p-value of lower than 0.05 was considered statistically significant. Univariate logistic regression was performed on each potential predictive variable, encompassing gender, age, pathological type, T stage, N stage, induction chemotherapy regimen and duration, tumour volume, synchronous chemotherapy duration, tumour or lymph node invasion of the carotid sheath, and duration of NPC progression. Variables with $p < 0.05$ were then included in multivariate binary logistic regression analyses to identify independent risk factors contributing to patient mortality. The selected risk factors and Rad-Score were utilized to construct a combined model, and a nomogram was generated. Following the model construction, the goodness of fit was analyzed using the Hosmer-Lemeshow test, and the decision curve analysis (DCA) diagram and ROC curve were plotted. The AUC served as an evaluation metric for the performance of each model in assessing the risk of death from NPC. The predictive performance of the models was compared using the Delong test, and a p-value of <0.05 indicated a statistically significant difference.

Results

Selection of Clinical Features and Semantic Features

NPC patients were divided into death group (n = 56) and non-death group (n = 54), based on their mortality status within 5 years of recurrence and/or distant metastasis. The Kappa values for cervical artery lymph node invasion and carotid sheath invasion were 0.826 and 0.909, respectively. Significant differences in gender ($p = 0.027$), invasion of the carotid sheath by primary tumour ($p < 0.001$), tumour volume ($p < 0.001$), and progression time ($p = 0.001$) were observed between the two groups, as shown in Table 1. Multivariate binary logistic regression showed that sex, tumour invasion of the carotid sheath, and tumour volume were all significant in predicting NPC death (Table 2). The forest plot of the multivariate binary logistic regression analysis is presented in Fig. 2.

Radiomic Features Selection

The mRMR method was used to select 20 texture features from a pool of 6858 features in the T1WI, FS T2WI, and FS CE-T1WI sequences. Then, the LASSO algorithm was applied to further optimize the selection process, retaining 8 optimal subsets (Fig. 3). The three features with the highest proportions were selected for inter-group analysis, as presented in Fig. 4.

Construction and Validation of the Combined Model

After five-fold cross-validation, each patient received five sets of Rad-Score values; the corresponding AUC values are displayed in Fig. 5A. The set with the highest AUC value was selected as the predictive model for radiomics. Considering the correlation between tumour volume and radiomics feature log_glszm_log-sigma-0-5-mm-3d-largearealowgraylevelemphasis, for the combined model, only

Table 1. Comparison of clinical and MRI semantic features between death and non-death groups.

Clinical and semantic features		Non-death (n = 54)	Death group (n = 56)	*p*	χ^2/Z
Sex	Male	38	49	0.027*	4.878
	Female	16	7		
Age (year)		51.500 (34.000, 68.000)	55.000 (46.000, 62.000)	0.054	–1.948
Pathological type	Type 1	10	7	0.743	——
	Type 2	27	25		
	Type 3	5	9		
	Type 4	1	1		
	Type 5	11	14		
Induction chemotherapy regimen	NO	6	8	0.883	0.249
	PF	28	28		
	TPF	20	20		
Course of induction chemotherapy	1	0	1	0.806	——
	2	2	1		
	3	52	54		
Synchronous course of chemotherapy	0	3	1	0.459	1.556
	1	3	5		
	2	48	50		
T stage	1	2	1	0.523	0.914
	2	3	3		
	3	30	30		
	4	19	22		
N stage	0	2	0	0.503	——
	1	17	17		
	2	24	23		
	3	11	16		

Table 1. Continued.

Clinical and semantic features		Non-death (n = 54)	Death group (n = 56)	*p*	χ^2/Z
Carotid sheath invasion	No	44	27	<0.001*	13.295
	Yes	10	29		
Lymph node invasion	No	30	24	0.183	1.774
	Yes	24	32		
Tumour volume	—	8069.000 (4860.5000, 15,096.667)	18,620.000 [6881.4167, 29,633.333)	<0.001*	–3.665
Progression time (years)	—	2.775 (1.6875, 3.750)	1.500 (1.000, 2.7125)	0.001*	–3.216

Note: * represents a statistically significant difference. Pathological types 1–5 represent squamous carcinoma, non-keratinizing undifferentiated carcinoma, non-keratinizing differentiated carcinoma, and basal cell-like carcinoma, respectively. NO, “No” and “Negative”; PF, platin and 5-fluorouracil; TPF, taxotere, platin and 5-fluorouracil; MRI, magnetic resonance imaging.

gender, carotid sheath invasion, duration of progression, and radiomics factors were included. ROC curves for the combined model are displayed in Fig. 5B. We also constructed DCA plots for the three models (Fig. 6). Accuracy, specificity, sensitivity, negative predictive value (NPV), and positive predictive value (PPV) were calculated for each mode, and the values are presented in Table 3. The Delong test was used to evaluate the differences between the models (Table 4). The results indicate that the radiomic feature outmatched the clinical semantic model with better performance in terms of death risk prediction, while the combined model had the best performance in this regard, with higher accuracy and stability than the other two models. We then established nomograms for all statistically different variables (Fig. 7). Finally, a fitted curve for the combined model was constructed (Fig. 8). The results showed a good match between the corrected predicted and the actual probability values.

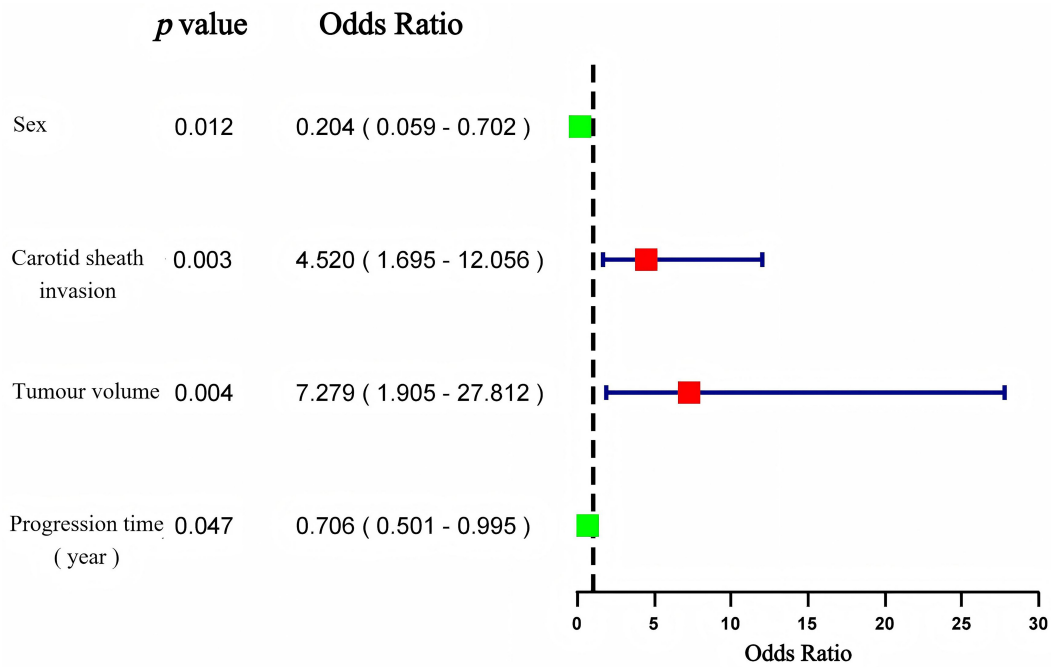

Fig. 2. Forest plot of multivariate binary logistic regression analysis. The red square indicates that the effect quantity is greater than 1, the green square indicates that the effect quantity is less than 1, and the error bar in blue indicates the corresponding confidence interval.

Discussion

In this study, we developed a clinical-semantic-radiomic nomogram for predicting the 5-year mortality risk in patients with progressive NPC. Our findings highlight that sex, tumour volume, carotid sheath invasion, and progression time are significant risk factors for death in patients with progressive NPC. Pre-treatment multi-parameter MRI radiomics boasts a great predictive power for NPC death, and combining it with clinical-sematic features provides the highest predictive efficacy

Table 2. Multivariate binary logistic regression between death and non-death groups.

Clinical and semantic features	β	SE	Wald χ^2	p	OR	95% CI
Sex	–1.589	0.631	6.352	0.012*	0.204	0.059–0.702
Carotid sheath invasion	1.509	0.500	9.085	0.003*	4.520	1.695–12.056
Tumour volume	1.985	0.684	8.424	0.004*	7.279	1.905–27.812
Progression time (year)	–0.348	0.175	3.963	0.047*	0.706	0.501–0.995

Note: * represents a statistically significant difference. The tumour volume data showed significant skewness and the presence of outliers. Therefore, we performed an exponential transformation on the volume data. SE, Standard Error; OR, Odds Ratio; CI, confidence interval.

Table 3. Evaluation indicators of each model.

Model	p	AUC	95% CI	Accuracy	Sensitivity	Specificity	NPV	PPV
Radiomic feature model	<0.001*	0.861	0.783–0.920	0.773	0.839	0.741	0.778	0.768
Clinical-semantic feature model	<0.001*	0.797	0.709–0.868	0.746	0.786	0.750	0.712	0.786
Combined model	<0.001*	0.904	0.832–0.952	0.818	0.857	0.870	0.778	0.857

Note: * represents a statistically significant difference. AUC, area under the curve; NPV, negative predictive value; PPV, positive predictive value.

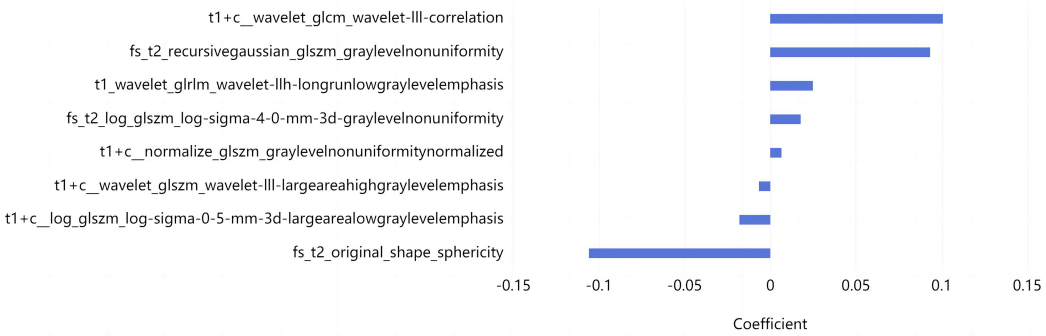

Fig. 3. Selected radiomics features. Eight radiomics features and their correlation coefficients between the death group and the non-death group were selected. The wavelet_glcm_wavelet-lll-correlation, glszm_graylevelnonuniformity and Original shape-sphericity make up the largest proportions. The wavelet_glcm_wavelet-lll-correlation in the T1WI-enhanced sequence provides insights into the consistency and variability of low-frequency texture features across the image. Higher correlation values suggest more consistent texture features between pixels, with the death group patients exhibiting higher values than those in the non-death group. The glszm_graylevelnonuniformity measures the variability of the intensity values in the image. Lower intensity values indicate higher homogeneity of intensity values. The death group clearly demonstrates higher values than the non-death group. Original shape-sphericity measures the roundness of the tumour region relative to a sphere; the smaller the value, the more the tumour tends to be spherical. The study results suggest that NPC patients with more irregular tumour shapes are at increased risk for mortality.

among the three models tested. The nomogram based on the combined model offers a quantitative tool for evaluating risks associated with early deaths from NPC.

The incidence of NPC is higher in male patients, and our research revealed that male patients with progressive NPC exhibit a poorer prognosis, aligning with the

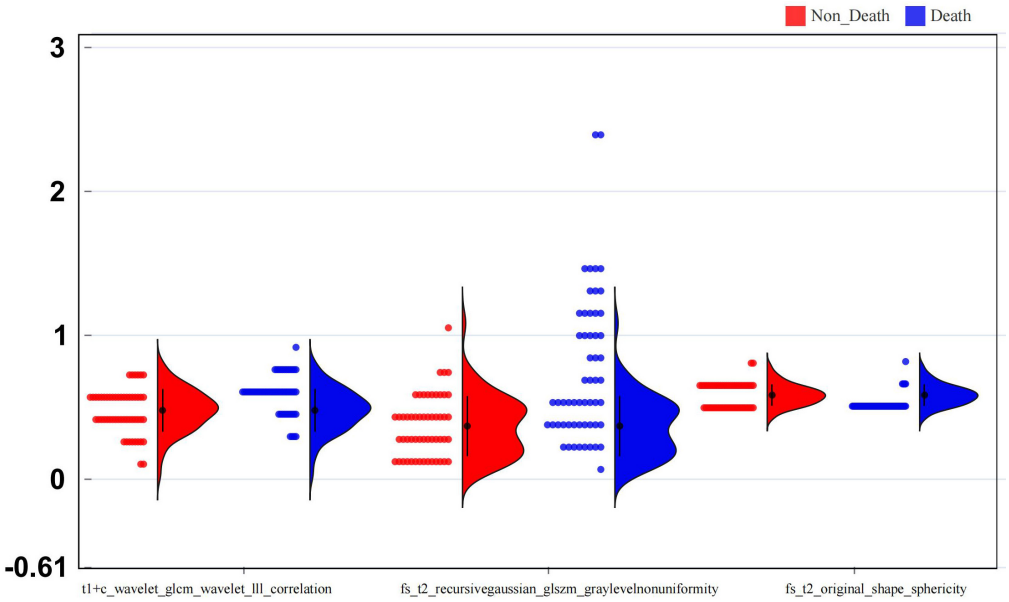

Fig. 4. Half violin plots depicting the distribution of three radiomic features with the highest proportion between the death group and non-death group. The left is a hive diagram, similar to a dithering scatter diagram, adding scatter effects along the y-axis. The right is a nuclear density graph, which yields an estimated probability density curve by placing a nuclear function around each data point and then stacking all the nuclear functions together. The y-axis represents the specific value of each point. In order to show the values corresponding to the three features on a single diagram, we reduced the second special value by 100 times.

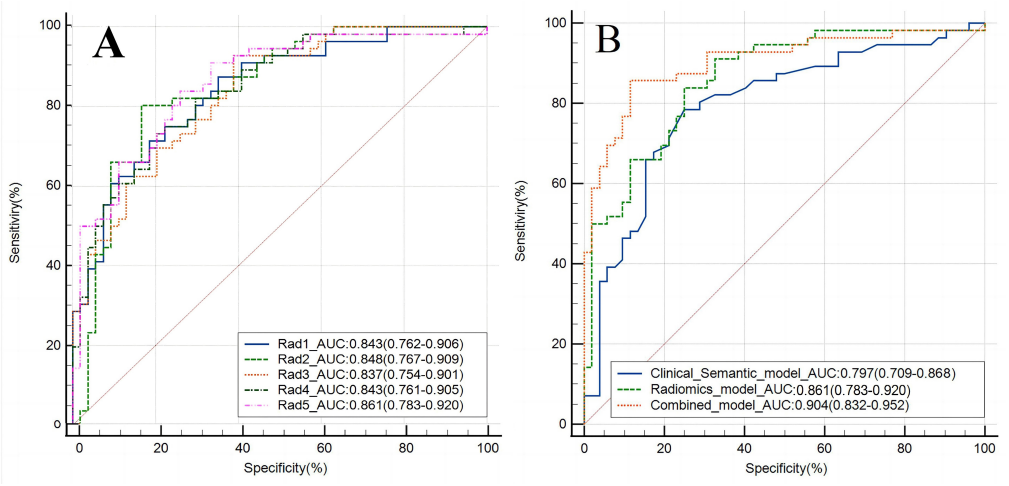

Fig. 5. ROC curves and corresponding AUC values for the three models. (A) ROC curve for the five-fold cross-validation of the Rad-Score in the death and non-death groups. Through five-fold cross-validation, the 5th model, also known as Rad 5, has an AUC value of 0.861, which is the highest, indicating the best performance. Clinical semantic features are then combined to build a combined model. (B) ROC curve for the combined model. AUC, area under the curve; ROC, receiver operating characteristic.

findings of Lu et al (2021). Additionally, Tian et al (2022) observed that patients with a primary tumour volume exceeding 30 cm^3 have a lower 5-year survival rate compared to those with a volume of less than 30 cm^3. Tumour size emerges as a

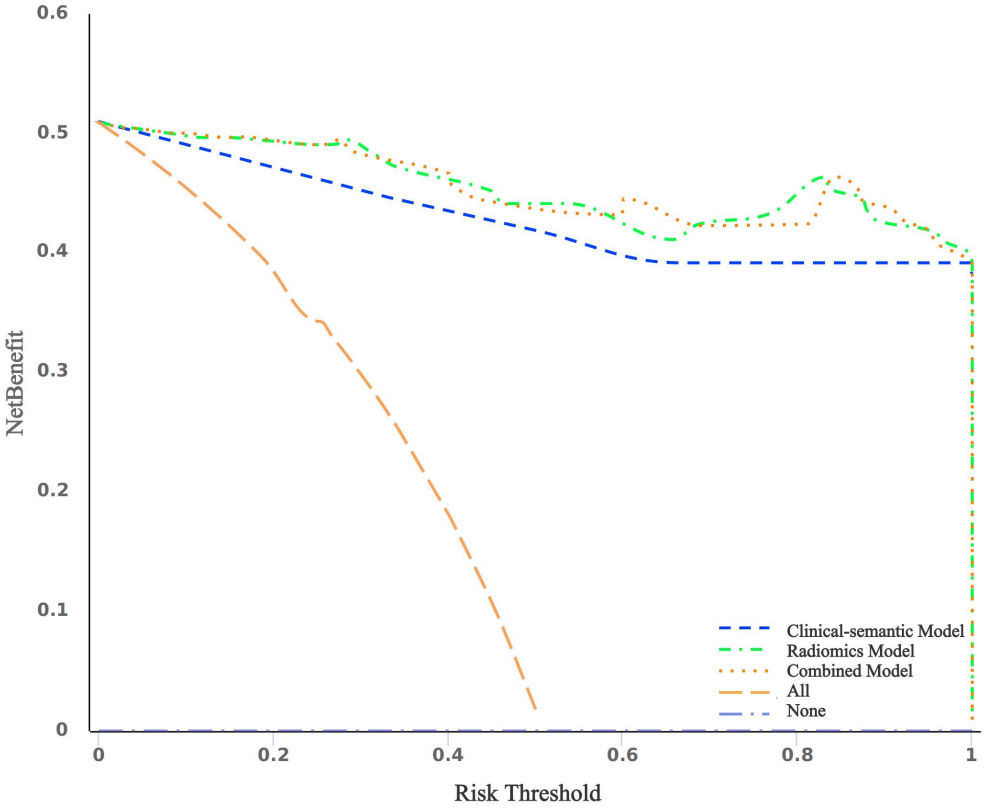

Fig. 6. Decision curves of the three models. The decision curve analysis (DCA) diagram shows that the radiomic feature model outperforms the clinical-semantic feature model in predicting death risk, while the combined model, incorporating clinical-semantic and radiomic features, has the best performance in this regard.

Table 4. Delong test of AUC values among three models.

	Radiomic feature model vs. clinical-semantic feature model	Radiomic feature model vs. combined model	Clinical-semantic feature model vs. combined model
Z	1.103	1.506	2.778
p	0.270	0.132	0.004*
95% CI	–0.049–0.176	–0.013–0.100	0.033–0.180

Note: * represents a statistically significant difference.

crucial factor in predicting distant metastasis and OS rates in the context of secondary IMRT (Xiao et al, 2015). Notably, carotid sheath invasion of blood vessels is considered a prognostic factor for negative survival outcomes (Lin et al, 2010; Rodrigues Dias et al, 2023). Larger tumour volume and invasion of the carotid sheath may result from a higher tumour burden, limiting the enhancement of radiotherapy dosing and influencing treatment effectiveness (Chen et al, 2019; Ni et al, 2020; Yan et al, 2022). Furthermore, our study also showed that time to tumour progression and death are closely related after precluding the tumour volume factor, and that the occurrence of earlier progression contributes to an increased risk of death.

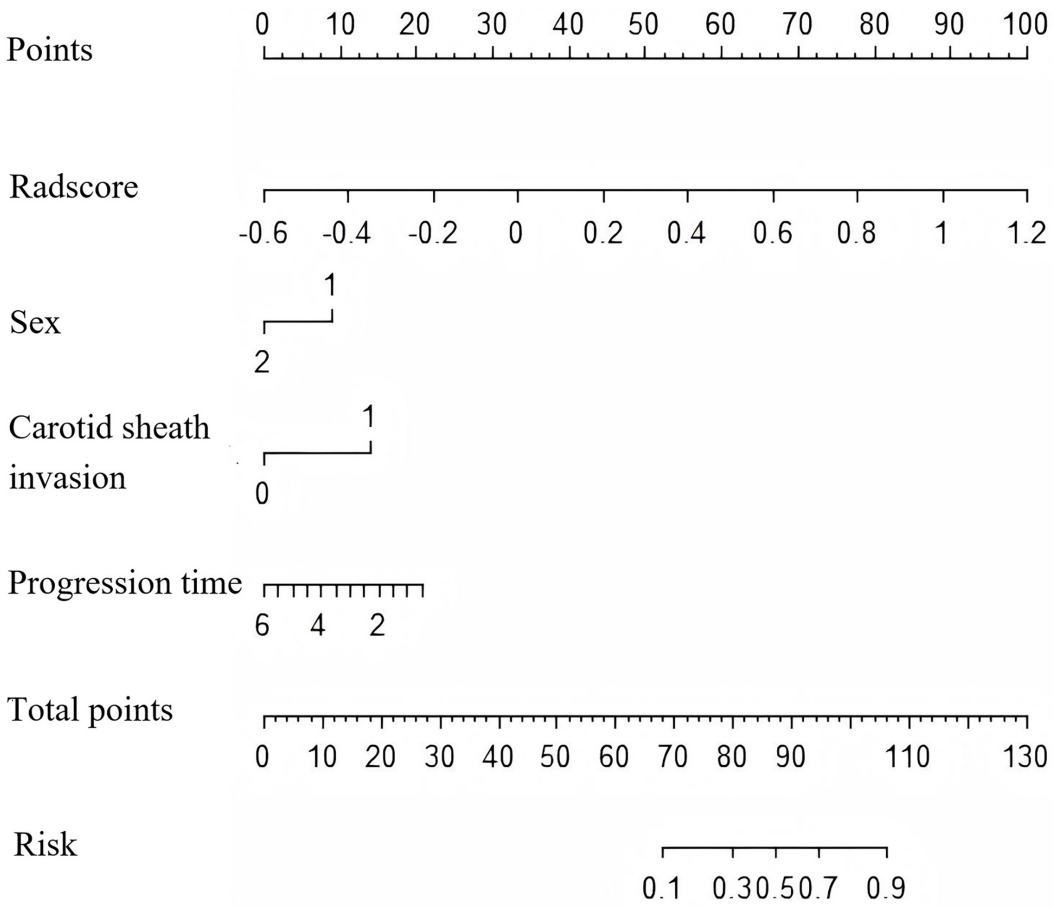

Fig. 7. Nomogram for comparing the death group and non-death group. For sex, 1 represents male, and 2 represents female; for carotid sheath invasion, 0 represents no tumour invading carotid sheath, and 1 represents tumour invasion. Each horizontal line represents an independent variable, and its length reflects the contribution of that variable to specific clinical outcomes by mapping these lines to the axis of the total score, a total score can be determined.

Tumour texture features are the primary optimal MRI features for the death group and the non-death group. Specifically, the wavelet_glcm_wavelet-lll-correlation in the T1WI in the death group is stronger than the correlation with patients in the non-death group. This observation may be attributed to the fact that most of the participants in this study had undifferentiated non-keratinizing NPC, characterized by a rich blood supply and rare tumour necrosis in the T1WI-enhanced sequence. The characteristic values of glszm_graylevelnonuniformity of the death group are significantly higher than those of the non-death group, indicating the involvement of a more pathologically heterogeneous primary tumour and its relation with a higher risk of death. Original shape-sphericity measures the roundness of the tumour region relative to a sphere. The study results suggest that NPC patients with more irregular tumour shapes are at an increased risk of mortality. This aligns with a previous study that suggested a correlation between more irregular tumour shapes, poorer tumour regression after treatment (Xi et al, 2022), and a higher risk of recurrence and metastasis (Xi et al, 2024).

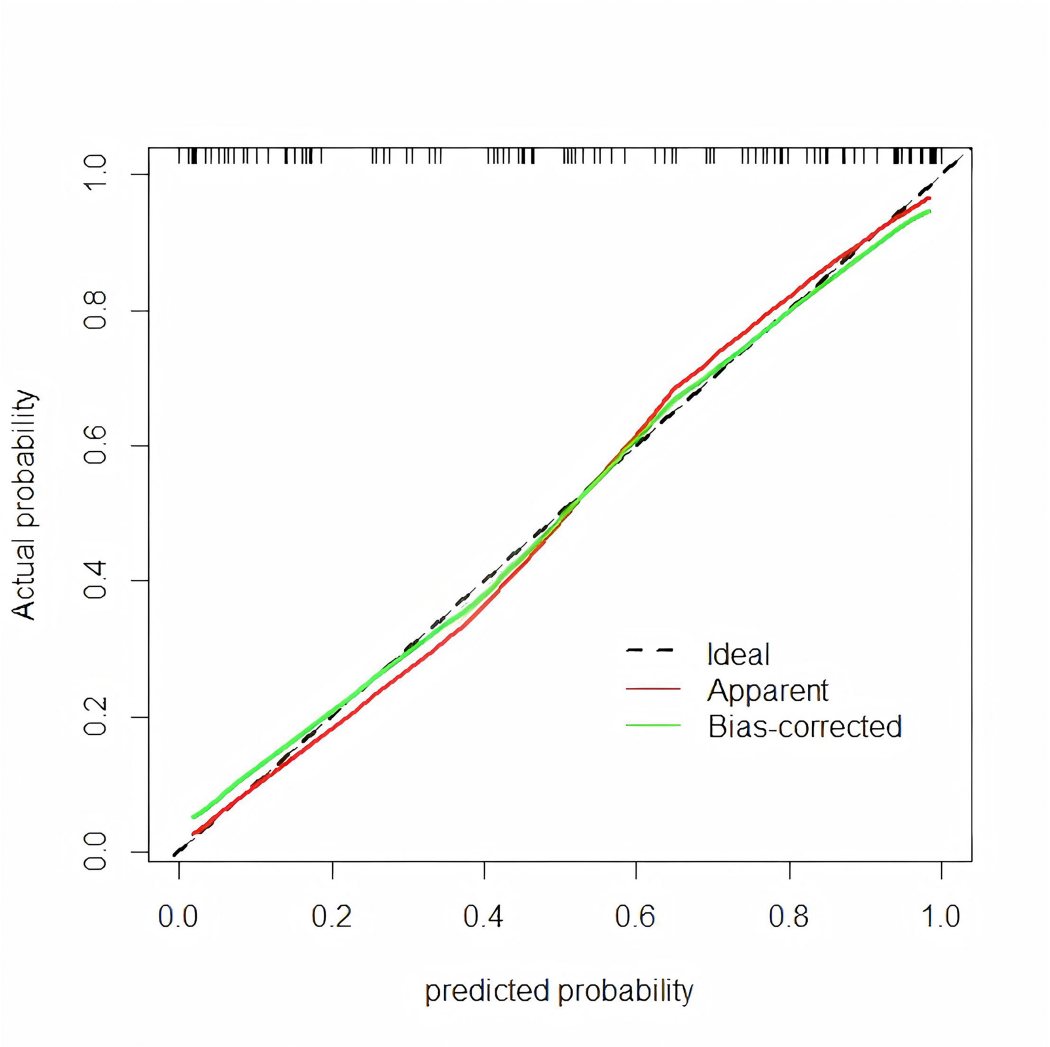

Fig. 8. Fitted curve comparing the death group and non-death group.

MRI is a traditional and important tool for aiding decision-making concerning treatments for NPC patients. The present study presents a multi-parameter MRI predictive model that includes longitudinal and transverse information about lesions. Incorporating clinical, imaging, and radiomics factors, the combined model provides an effective prediction of death risk in patients with advanced NPC. A nomogram based on the combined model was established to stratify patients with recurrence and/or distant metastasis at an early stage. Since high-risk patients suffer from higher degrees of tumour heterogeneity, larger tumour burden, and earlier disease progression, we recommend implementing intensive intervention measures in the initial treatment stage and increasing imaging reviews in the later stages of follow-up.

However, our study is not without limitations: (1) It is a retrospective analysis, inherently subject to selection bias. (2) The data were derived from a single center, and the sample was small. Thus, future studies should include multi-center data for enhancing model generalizability. (3) Our data for both the death group and the

non-death group are relatively small. We will strive to follow up and collect more data in the later stages to verify the reliability of our model.

Conclusion

A comprehensive model integrating multivariate imaging data from pre-treatment multi-parameter MRI radiomics, clinical-semantic, and MRI features can accurately predict the survival outcome of individuals with progressive NPC. This combined model boasts heightened accuracy of predicting mortality risk associated with NPC. Stratification based on high-risk factors offers a high-throughput and non-invasive quantitative assessment basis for early intervention and timely optimization of treatment plans. Thus, this model may help with achieving a balance between survival benefits and medical costs.

Key Points

- The survival rate among patients with recurrent or/and metastatic NPC is notably low.
- Sex, tumour volume, carotid sheath invasion, and progression time are significant risk factors for death in patients with progressive NPC.
- Pre-treatment multi-parameter MRI radiomics exhibit substantial predictive efficacy for NPC-related mortality.
- Among the three models tested, the combined model incorporating clinical-semantic features and multi-parameter MRI radiomic features boasts the highest efficacy in predicting death risk in patients with progressive NPC.

Availability of Data and Materials

The datasets used and/or analyzed during the current study are available from the corresponding author upon reasonable request.

Author Contributions

Study concepts: FJ, ZD; Study design: FJ, ML; Definition of intellectual content: YX, MW; Data analysis: YX, CW, MW, YD, LR; Statistical analysis: YZ, YX, XC; Manuscript drafting: YX; Manuscript review and guarantor of the integrity of the entire study: YX. All authors contributed to important editorial changes in the manuscript. All authors read and approved the final manuscript. All authors have participated sufficiently in the work and agreed to be accountable for all aspects of the work.

Ethics Approval and Consent to Participate

The research involving human participants was conducted by the 903th RD Hospital of PLA. This study was approved by the 903th RD Hospital of PLA research ethics committee (Approval No. 20220722/08/01/00). Acquisition of informed consent of study participants was waived since the study did not implement

interventions that would harm the subjects (physical, mental, social status, etc.), did not involve personal and private data, and did not entail commercial interests, as well as the data were collected a relatively long time ago (before 2022).

Acknowledgement

Not applicable.

Funding

This research is supported by Natural Science Foundation of Zhejiang Province (Y22H185692), Medical Science and Technology Project of Zhejiang Province (NO. 2023KY209, NO. 2022KY1047), and Hangzhou Science and Technology Commission (NO. B20241726).

Conflict of Interest

The authors declare no conflict of interest.

References

Chan JYW, Wong STS, Wei WI. Stage II recurrent nasopharyngeal carcinoma: Prognostic significance of retropharyngeal nodal metastasis, parapharyngeal invasion, and carotid encasement. Head & Neck. 2018; 40: 103–110. https://doi.org/10.1002/hed.24976

Chen FP, Wen DW, Li F, Lin L, Kou J, Zheng WH, et al. The Role of Post-Neoadjuvant Chemotherapy Tumor Volume for Prognostication and Treatment Guidance in Loco-Regionally Advanced Nasopharyngeal Carcinoma. Cancers. 2019; 11: 1632. https://doi.org/10.3390/cancers11111632

Chen S, Yang D, Liao X, Lu Y, Yu B, Xu M, et al. Failure Patterns of Recurrence and Metastasis After Intensity-Modulated Radiotherapy in Patients With Nasopharyngeal Carcinoma: Results of a Multicentric Clinical Study. Frontiers in Oncology. 2022; 11: 693199. https://doi.org/10.3389/fonc.2021.693199

de Martel C, Georges D, Bray F, Ferlay J, Clifford GM. Global burden of cancer attributable to infections in 2018: a worldwide incidence analysis. The Lancet. Global Health. 2020; 8: e180–e190. https://doi.org/10.1016/S2214-109X(19)30488-7

Deng Y, Huang Y, Jing B, Wu H, Qiu W, Chen H, et al. Deep learning-based recurrence detector on magnetic resonance scans in nasopharyngeal carcinoma: A multicenter study. European Journal of Radiology. 2023; 168: 111084. https://doi.org/10.1016/j.ejrad.2023.111084

Huang SH, O'Sullivan B. Overview of the 8th Edition TNM Classification for Head and Neck Cancer. Current Treatment Options in Oncology. 2017; 18: 40. https://doi.org/10.1007/s11864-017-0484-y

Lin S, Lu JJ, Han L, Chen Q, Pan J. Sequential chemotherapy and intensity-modulated radiation therapy in the management of locoregionally advanced nasopharyngeal carcinoma: experience of 370 consecutive cases. BMC Cancer. 2010; 10: 39. https://doi.org/10.1186/1471-2407-10-39

Liu Y, Li H, Zeng T, Wang Y, Zhang H, Wan Y, et al. Integrated bulk and single-cell transcriptomes reveal pyroptotic signature in prognosis and therapeutic options of hepatocellular carcinoma by combining deep learning. Briefings in Bioinformatics. 2023; 1: bbad487. https://doi.org/ 10.1093/bib/bbad487

Lu ZJ, Liu LT, Sun XS, Guo SS, Yang Q, Liu SL, et al. Establishment and validation of a prognostic nomogram to predict early metastasis in nasopharyngeal carcinoma patients within six months after radiotherapy and to guide intensive treatment. Radiotherapy and Oncology. 2021; 162: 202–211. https://doi.org/10.1016/j.radonc.2021.03.035

Miao S, Lei H, Li X, Zhou W, Wang G, Sun A, et al. Development and validation of a risk prediction model for overall survival in patients with nasopharyngeal carcinoma: a prospective cohort study in China. Cancer Cell International. 2022; 22: 360. https://doi.org/10.1186/s12935-022-02776-8

Ni W, Qi W, Xu F, Cao W, Xu C, Chen J, et al. Prognostic value of nasopharynx tumour volume in local-regional advanced nasopharyngeal carcinoma. Annals of Translational Medicine. 2020; 8: 223. https://doi.org/10.21037/atm.2020.01.03

Qiang M, Li C, Sun Y, Sun Y, Ke L, Xie C, et al. A Prognostic Predictive System Based on Deep Learning for Locoregionally Advanced Nasopharyngeal Carcinoma. Journal of the National Cancer Institute. 2021; 113: 606–615. https://doi.org/10.1093/jnci/djaa149

Qiu W, Zhong X, Jiang J, Huang L, Li J, Zheng R, et al. Prognostic significance of cervical radiologic carotid artery invasion by lymph node on magnetic resonance imaging in nasopharyngeal carcinoma. Cancer Imaging. 2023; 23: 26. https://doi.org/10.1186/s40644-023-00544-z

Quan T, Guan W, Huang W, Cui C, Li H, Ruan G, et al. Carotid space involvement is a prognostic factor and marker for induction chemotherapy in patients with nasopharyngeal carcinoma. Oral Oncology. 2022; 135: 106230. https://doi.org/10.1016/j.oraloncology.2022.106230

Ren Y, Qiu H, Yuan Y, Ye J, Tian Y, Wen B, et al. Evaluation of 7th Edition of AJCC Staging System for Nasopharyngeal Carcinoma. Journal of Cancer. 2017; 8: 1665–1672. https://doi.org/10.7150/jca.19197

Rodrigues Dias D, Breda E, Sousa F, Soares A, Monteiro E. Nasopharyngeal carcinoma in a non-endemic country-Validation of the new NPC staging system. Acta Otorrinolaringologica Espanola. 2023; 74: 39–49. https://doi.org/10.1016/j.otoeng.2022.04.001

Siak PY, Khoo ASB, Leong CO, Hoh BP, Cheah SC. Current Status and Future Perspectives about Molecular Biomarkers of Nasopharyngeal Carcinoma. Cancers. 2021; 13: 3490. https://doi.org/10.3390/cancers13143490

Sung H, Ferlay J, Siegel RL, Laversanne M, Soerjomataram I, Jemal A, et al. Global Cancer Statistics 2020: GLOBOCAN Estimates of Incidence and Mortality Worldwide for 36 Cancers in 185 Countries. CA: A Cancer Journal for Clinicians. 2021; 71: 209–249. https://doi.org/10.3322/caac.21660

Tian Y, Huang WZ, Zeng L, Bai L, Han F, Lan Y. The Failure Patterns of Nasopharygeal Carcinoma After Intensity-Modulated Radiotherapy and Implications for Surveillance. Cancer Management and Research. 2022; 14: 2813–2823. https://doi.org/10.2147/CMAR.S347864

Toumi N, Ennouri S, Charfeddine I, Daoud J, Khanfir A. Local and Lymph Node Relapse of Nasopharyngeal Carcinoma: A Single-Center Experience. Ear, Nose, & Throat Journal. 2021; 100: 795S–800S. https://doi.org/10.1177/0145561320908955

Wu S, Li H, Dong A, Tian L, Ruan G, Liu L, et al. Differences in Radiomics Signatures Between Patients with Early and Advanced T-Stage Nasopharyngeal Carcinoma Facilitate Prognostication. Journal of Magnetic Resonance Imaging. 2021; 54: 854–865. https://doi.org/10.1002/jmri.27633

Xiang AY, Wang KH, Su W, Tan T, Qu YF, Li XQ, et al. Endoscopic resection of giant esophageal subepithelial lesions: experience from a large tertiary center. Gastrointestinal Endoscopy. 2024; 3: 358–370.e11. https://doi.org/10.1016/j.gie.2023.10.032.

Xiao W, Liu S, Tian Y, Guan Y, Huang S, Lin C, et al. Prognostic significance of tumor volume in locally recurrent nasopharyngeal carcinoma treated with salvage intensity-modulated radiotherapy. PLoS ONE. 2015; 10: e0125351. https://doi.org/10.1371/journal.pone.0125351

Xi Y, Dong H, Wang M, Chen S, Han J, Liu M, et al. Early prediction of long-term survival of patients with nasopharyngeal carcinoma by multi-parameter MRI radiomics. European Journal of Radiology Open. 2024; 12: 100543. https://doi.org/10.1016/j.ejro.2023.100543

Xi Y, Ge X, Ji H, Wang L, Duan S, Chen H, et al. Prediction of Response to Induction Chemotherapy Plus Concurrent Chemoradiotherapy for Nasopharyngeal Carcinoma Based on MRI Radiomics and Delta Radiomics: A Two-Center Retrospective Study. Frontiers in Oncology. 2022; 12: 824509. https://doi.org/10.3389/fonc.2022.824509

Yan G, Feng Y, Wu M, Li C, Wei Y, Hua L, et al. Prognostic significance of MRI-based late-course tumor volume in locoregionally advanced nasopharyngeal carcinoma. Radiation Oncology. 2022; 17: 111. https://doi.org/10.1186/s13014-022-02087-2

Yang K, Tian J, Zhang B, Li M, Xie W, Zou Y, et al. A multidimensional nomogram combining overall stage, dose volume histogram parameters and radiomics to predict progression-free survival in patients with locoregionally advanced nasopharyngeal carcinoma. Oral Oncology. 2019; 98: 85–91. https://doi.org/10.1016/j.oraloncology.2019.09.022

Zhang L, Dong D, Li H, Tian J, Ouyang F, Mo X, et al. Development and validation of a magnetic resonance imaging-based model for the prediction of distant metastasis before initial treatment of nasopharyngeal carcinoma: A retrospective cohort study. eBioMedicine. 2019; 40: 327–335. https://doi.org/10.1016/j.ebiom.2019.01.013

Zhuo EH, Zhang WJ, Li HJ, Zhang GY, Jing BZ, Zhou J, et al. Radiomics on multi-modalities MR sequences can subtype patients with non-metastatic nasopharyngeal carcinoma (NPC) into distinct survival subgroups. European Radiology. 2019; 10: 5590–5599. https://doi.org/10.1007/s00330-019-06075-1